Vapor phase SiO_2 etching and metallic contamination removal in an integrated cluster system

Y. Ma,[a] M. L. Green, L. C. Feldman, J. Sapjeta, K. J. Hanson, and T. W. Weidman
AT&T Bell Laboratories, Murray Hill, New Jersey 07974

(Received 7 March 1995; accepted 6 May 1995)

Vapor phase pregate oxide surface preparation was studied in a high vacuum cluster tool. SiO_2 was etched with anhydrous vapor hydrogen fluoride and methanol vapor. The oxide etch rate can be well controlled by varying wafer temperature, chamber pressure, and gas flow rates. A standard error of 5% in oxide etch rate has been achieved. Particles generated are less than ten per 125 mm wafer at an oxide etch rate of 60 Å/min. Atomic force microscopy measurements reveal no added Si surface microroughness attributable to vapor hydrogen flouride (HF) etching. Trace metallic contaminants such as iron and chromium were reduced with UV/Cl_2 based processes. A combination of vapor HF etching followed by UV/Cl_2 metal removal is an effective pregate oxide surface preparation. © *1995 American Vacuum Society.*

I. INTRODUCTION

One of the most important processes in modern integrated circuit (IC) manufacturing is pregate oxide wafer surface preparation. It has been shown that the performance of metal-oxide-semiconductor (MOS) devices depends on the cleaning processes prior to gate oxide growth.[1–5] However, with the traditional manufacturing processes, wafers are transferred from tool to tool within a clean room after each process, therefore exposing them to the risk of recontamination. For some critical process sequences such as gate oxide growth, the oxide should be grown immediately after wafer cleaning in order to reduce oxide defects and achieve high device yield.

To achieve contamination-free manufacturing, clustering is one of the options. Cluster tools allow single wafer processing during which wafers are transferred under vacuum between process modules and the risk of recontamination is reduced. Equipped with *in situ* diagnostics, process stability can be better controlled. Single wafer processing becomes more and more attractive with larger wafer size. Vacuum compatible, vapor phase cleaning processes are currently receiving much attention.[6–9] During vapor phase processes, oxides and other surface contaminants may be removed by reactions between reactive gases and surface layers/contaminants. Vapor phase processing also has the potential to clean smaller features, since wet processing is limited by solution surface tension. An additional advantage of vapor phase processing is the reduced chemical consumption compared to wet batch processing. As a result, vapor phase processing is environmentally friendly.

As an example, Table I summarizes data collected from our research facility. Data indicate an average of the pregate oxide cleaning process for one month period. As can be seen, except for HF, a direct comparison is difficult since chemicals used in the two schemes are basically different. However, we have observed that (1) the amount of HF consumed in vapor phase cleaning is about six times less than that in wet cleaning, (2) a very large amount of de-ionized (DI) water is consumed during the wet batch process, and (3) the amount of chemicals consumed in vapor phase cleaning is small, compared to wet cleaning.

Besides the effectiveness of vapor phase processing itself, success of vapor phase processing depends on large-scale implementation of single wafer processing technology. We conclude in this article and others[6–11] that vapor phase processing is promising for pregate oxide cleaning. The adoption of the minienvironment concept in clean rooms will lead to more single wafer processing tools in manufacturing. This, combined with stricter regulations on hazardous chemical consumption and disposal, will accelerate the implementation of the technology.

In this article, we report our study of vapor hydrogen fluoride etching of SiO_2 and ultraviolet assisted cleaning in a high vacuum integrated system. We present data on oxide etching, surface microroughness, particle generation during cleaning, and metallic contamination removal. We have also investigated the electrical properties of gate oxides and the SiO_2/Si interface formed by vapor phase cleaning and rapid thermal oxidation. Those results have been summarized in a recent article, to be published elsewhere.[12]

II. CLUSTER TOOL

The cluster tool (Fig. 1) used for this study is composed of four chambers: Submicron Primaxx for vapor phase cleaning, AG Integra One for rapid thermal oxide growth, a central wafer handler (robot) chamber, and a load lock chamber.

The cleaning chamber (Fig. 2) is made of aluminum oxide (Al_2O_3) to resist corrosion by reactive gases (hydrogen fluoride and chlorine). It can handle 125–200 mm diam wafers. Wafers can be heated up to 250 °C by four infrared lamps. Temperature is monitored by a pyrometer aimed at the backside of the wafer, and controlled by a computer. UV radiation is generated by a xenon lamp with a broadband wavelength. Wafers are supported by a magnetically floating tripod and rotated during processing to give maximum uniformity across the wafer surface. HF vapor, O_2, Cl_2, and N_2 gases flow directly into the chamber, while methanol is brought

[a]Present address: AT&T Bell Laboratories, 9333 S. John Young Pkwy., Orlando, FL 32819.

TABLE I. Comparison of chemical consumption for conventional wet/batch cleaning and vapor phase/single wafer cleaning.

Chemicals	Wet cleaning (10^{-3} ℓ/wafer)	Vapor phase cleaning (10^{-3} ℓ/wafer)
HF	4.2	0.7
H_2SO_4	106.2	0
H_2O_2	26.7	0
DI H_2O	31 416	0
CH_3OH	0	0.17
Cl_2	0	0.19
O_2	0	1.15
N_2	0	1.72

into the chamber by bubbling N_2 through it. The amount of methanol is adjusted by varying the N_2 flow rate. All gases introduced into the chamber are of semiconductor grade and filtered to insure ultra purity and cleanliness.

III. CLEANING MECHANISMS

Our vapor phase pre-gate oxide preparation consists of three chemical processes: (i) etching in anhydrous vapor hydrogen fluoride and methanol to remove (native or sacrificial) oxide; (ii) UV/O_3 ($UV+O_2$) to remove hydrocarbon contaminants, and (iii) UV/Cl_2 to reduce trace metal contaminants. The combination of the three processes will result in a clean, dry, particle, and damage-free surface, ideal for gate oxide growth.

In a conventional aqueous HF process, SiO_2 etching occurs when the highly polar HF molecule attacks the highly polar Si–O bonds by insertion between the Si and O atoms. This leads to cleaving of Si–O–Si bonds along with formation of thermodynamically stable products, such as SiF_4. The reaction can be expressed as

$$SiO_2+4HF\xrightarrow{OH}SiF_4+2H_2O. \quad (1)$$

In the case of the vapor HF/methanol (CH_3OH) chemistry, polarization is provided by hydroxyl groups of methanol

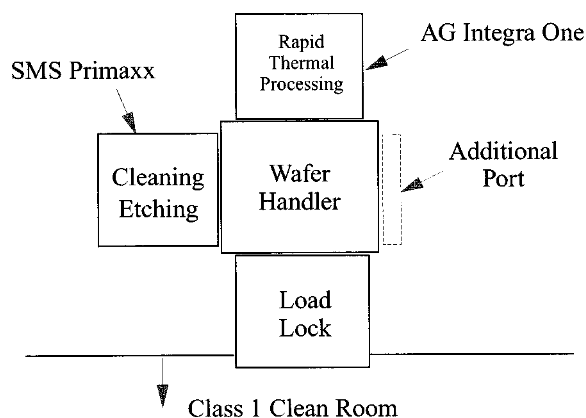

FIG. 1. Schematic of the high vacuum cluster tool used in this study. The four chamber system includes a vapor phase clean process chamber, rapid thermal oxidation chamber, wafer handler chamber, and load-lock chamber.

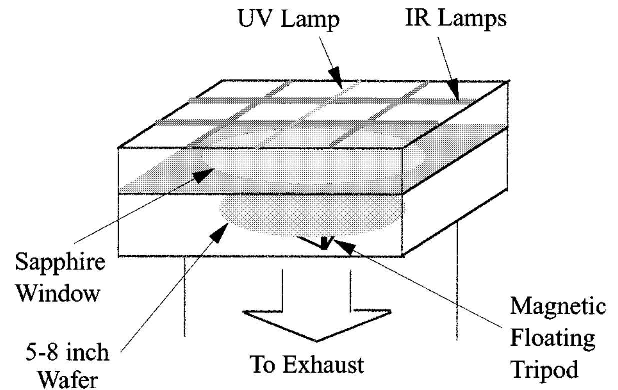

FIG. 2. The vapor phase process chamber. The chamber is made of aluminum oxide (Al_2O_3) and is capable of processing wafer sizes of 125–200 mm. The sapphire window allows wafers to be heated by four infrared lamps. Ozone and chlorine radicals are generated by a broad band xenon UV lamp.

molecules. However, the polarization is not as strong as that provided by water and oxide etch rates are generally slower than in the HF/H_2O system.

As mentioned by Helms *et al.*,[13] it is necessary to form a condensed layer on wafer surface to initiate an etching process the same as wet chemical etching where wafer surface is in a constant contact with the solution. In the case of vapor HF/methanol, the condensed layer is expected to be thinner than the vapor HF/H_2O system because of a higher methanol vapor pressure. However, the authors did notice that etching (at a very low etch rate) still takes place at a temperature of 100 °C at which no condensation is expected.

In the UV/O_3 processing, oxygen entering the reaction chamber is exposed to UV light causing its partial conversion to ozone (O_3). With absorption of another photon, UV generated ozone can further react to release atomic oxygen. This atomic oxygen reacts with hydrocarbons absorbed on the surface to form CO_2 and water, which desorbs from the wafer surface. Additional oxidation of Si forms a SiO_2 thin film. The processes are

$$(4y+xy)O+2(CH_x)_y\rightarrow 2yCO_2+xyH_2O, \quad (2)$$

$$2O+Si\rightarrow SiO_2. \quad (3)$$

In the metallic contamination removal process, chlorine radicals formed by UV activation of chlorine molecules react with surface metal atoms to form chloride complexes which are volatile and desorb from the wafer surface

$$xCl\cdot+M\rightarrow MCl_x, \quad (4)$$

where $Cl^{\cdot}$ is a chlorine radical, x is any integer, and M represents a metal atom or metal oxide molecule.

IV. EXPERIMENTAL PROCEDURES

Substrates used were 125 mm Si(100) wafers, boron doped to a resistivity of 10–20 Ω cm. For oxide etching studies, 1200 Å oxides were grown in a furnace at a temperature of 1000 °C in an O_2 atmosphere. Wafers were loaded into the cluster tool load lock after a wet chemical cleaning, which consisted of H_2SO_4:H_2O_2=12.5:1 at 105 °C

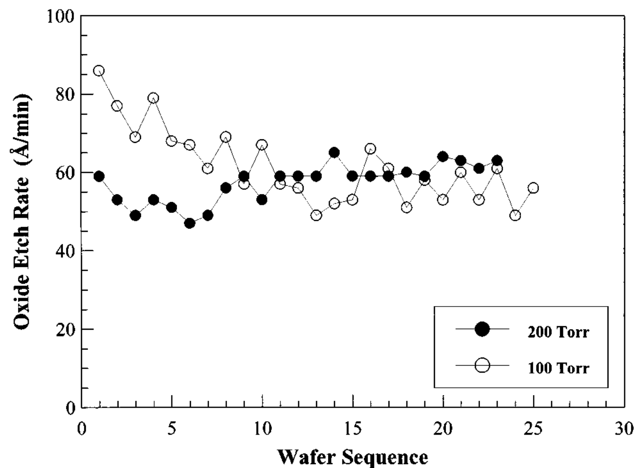

FIG. 3. Oxide etch rate as a function of wafer sequence from two cassettes processed at chamber pressures of 100 and 200 Torr, respectively. The decreasing etch rate trend for the first several wafers at 100 Torr was due to an uncontrollable flow of methanol into the chamber.

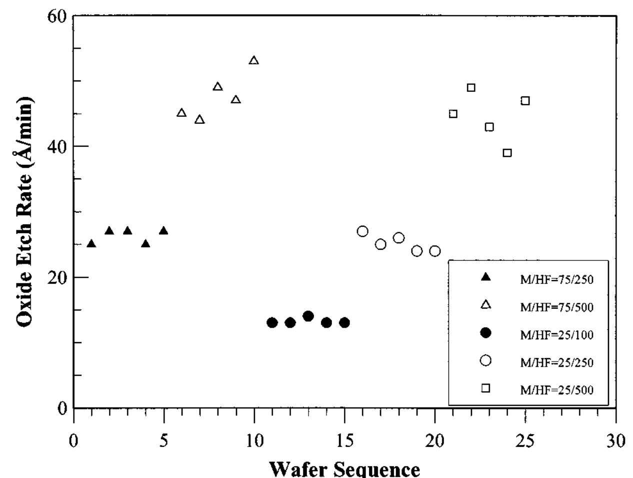

FIG. 4. Oxide etch rate from a cassette of wafers processed with five different recipes, five wafers per each recipe. Legend indicates flow rate ratio of methanol to vapor HF.

for 10 min, followed by 100:1 HF for 2 min, DI water rinse and a spin dry. Reactive gases used for SiO_2 etching were vapor HF and methanol. The gas flow rates were in the range of 100–500 sccm for vapor HF, 50–300 sccm for methanol (carrier gas, N_2), and 300–1000 sccm for N_2, respectively. Process temperature was 20–80 °C and pressure was 100–500 Torr. Oxide thickness was measured with a Rudolph ellipsometer and a Nano-Spec 2100 interferometer. Particles of size greater than 0.2 μm were measured with a Tencor 6100. Silicon surface morphology after vapor HF etching was characterized with atomic force microscopy (AFM) using a Nanoscope III in tapping mode with etched Si tips.

In the metallic contaminants removal study, silicon wafers were first intentionally contaminated with photoresist spun on the surface and then baked dry. The dried photoresist was subjected to an oxygen plasma ashing process. Bulk photoresist was removed, leaving behind a surface contaminated with chromium at a concentration of $1\times10^{12}/cm^2$ and iron at $3-4\times10^{11}/cm^2$. Both metal surface concentrations were characterized with total reflection x-ray fluorescence (TXRF). The cleaning efficiency was measured by the metal surface concentration difference before and after the cleaning processes.

V. RESULTS AND DISCUSSIONS

A. SiO_2 etching

We first present results of oxide etching. The dependence of the oxide etch rate on process parameters such as gas mixture, temperature, and chamber pressure has been reported by various authors.[7,10,11] Our results agree well with those studies. We emphasize here the tool's reliability and capability. Figure 3 shows SiO_2 etch rates from two cassettes of wafers, etched at two different chamber pressures, 100 and 200 Torr, respectively. At 100 Torr, the etch rate decreases for the first few wafers and then stabilizes. The decrease is caused by an unstable flow of methanol. Higher methanol flow rate normally results in greater oxide etch rate. At room temperature, the methanol vapor pressure is about 100 Torr. When the chamber pressure is set at about 100 Torr, the methanol delivery system allows some additional methanol to flow into the chamber. The uncontrolled influx of methanol can be reduced by increasing the chamber pressure to 200 Torr or higher. By raising the chamber pressure, the amount of methanol flowing into the chamber is well controlled, thus stabilizing the oxide etch rate. The standard error of etch rates for the cassette processed at 200 Torr is about 5.0%. The tool also has the capability of processing different wafers in a cassette with different recipes. One such case is presented in Fig. 4, which shows the oxide etch rate variation in a cassette of 25 wafers processed with five different recipes. The tool responds well to the variation of process parameters and for each recipe the oxide etch rate is repeatable from wafer to wafer. It can also be seen that the oxide etch rate increases with increasing vapor HF flow rates. However, the higher the etch rate, the greater is the variation in oxide etch rate.

To find a process window where the tool gives an optimum performance of oxide etching, a design of experiment was conducted. One result from the experiment is shown in Fig. 5, where the oxide etch rate standard error is plotted as a function of the oxide etch rate. Each data point in the figure represents one recipe with five wafers processed. The etch rate variation increases with increasing etch rate. There is a process window where a variation less than 5% can be achieved. As can be seen, three of the recipes have been repeated and confirmed. With careful design of the process, smaller variation can be realized. To control the repeatability from wafer to wafer, an etch rate less than 100 Å/min is desirable.

B. Surface morphology

Si/SiO_2 interfacial roughness usually results in higher leakage current or early dielectric breakdown of SiO_2 dielectric films.[14,15] Si surface microroughness can be increased

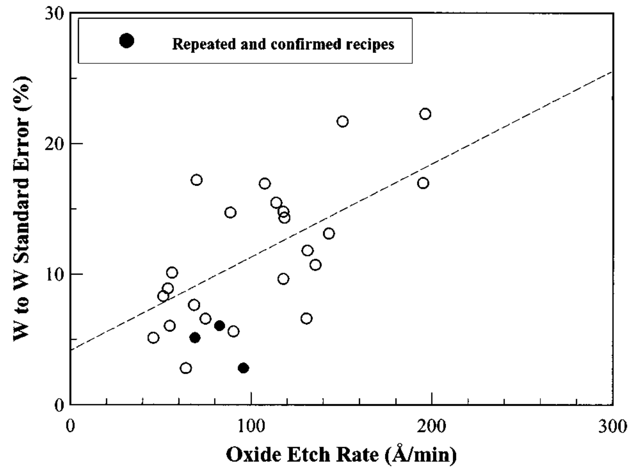

FIG. 5. Oxide etch rate standard error as a function of oxide etch rate. Each data point represents a five wafer average.

during HF etching, chemical cleaning and even DI water rinse.[15–18] An atomically smooth surface is ideal for gate oxide formation.

As discussed above, the oxide etch rate fluctuates in the vapor HF oxide etching process. Overetching is required to guarantee a complete removal of the sacrificial oxide. Surface roughness due to the overetching is not desirable. Figure 6(a) is an AFM image from a Si(100) surface aggressively etched by vapor HF. The etching took place at 50 °C, and at a chamber pressure of 200 Torr for a period of 3 min, equivalent to an oxide etch rate of 60 Å/min. The root-mean-square (rms) roughness of this surface is 0.24 nm. As a comparison, the result from a Si(100) surface etched with 100:1 aqueous HF for 2 min is shown in Fig. 6(b). Here, the rms value is 0.26 nm. Therefore, no difference has been observed between vapor and aqueous HF etched Si(100) surfaces.

C. Particle generation during SiO_2 etching

Particles on the Si surface affect electrical performance of MOS devices. They can increase SiO_2/Si interface trap density if they stay at the interface. Further, they can cause higher leakage current at low electrical field if they imbed themselves in the bulk of the oxide, since these sites provide an additional channel for current conduction.[19]

In the wet cleaning and DI water rinse processes, particles may float on top of the liquid. There is a potential that some of them redeposit on the surface of the wafers while pulling wafers out of the solution. One of the advantages of vapor phase processing is that no DI water rinse is involved. All reaction by-products should be vaporized and desorbed from the surface.

Particles can form from reaction by-products. In the case of SiO_2 etching, $H_2Si_2F_6$ can be present as particles. Its decomposition to the more volatile species SiF_4 is critical for a low particle generation process. Particle generation is controlled by the by-product generation rate and desorption rate. If the generation rate is larger than the desorption rate, particles will accumulate. The generation rate is directly related to the oxide etch rate while the desorption rate can be controlled by varying process temperature and pressure. Normally, higher substrate temperature and lower process pressure favors by-product desorption.

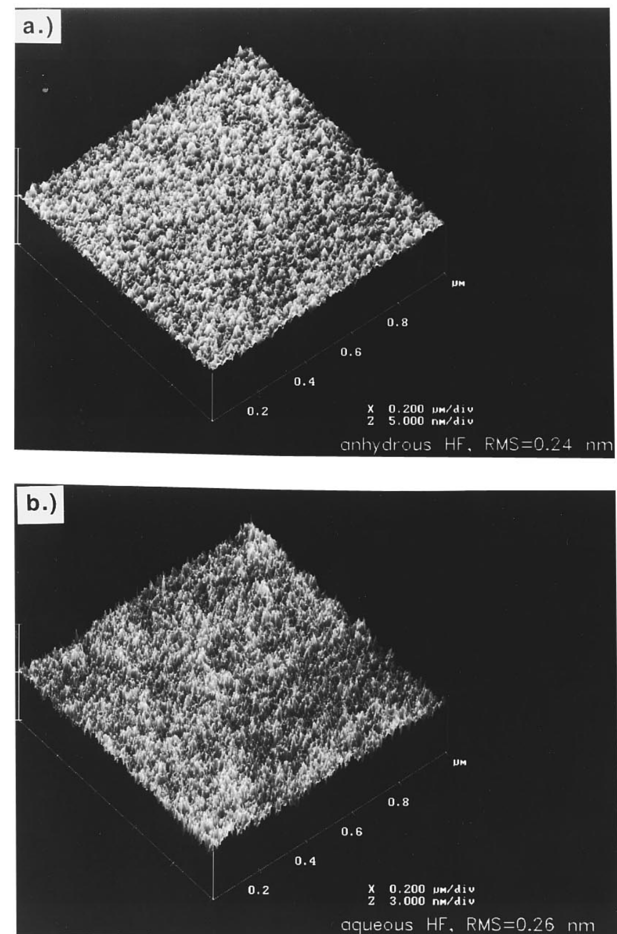

FIG. 6. AFM images from a Si(100) surface etched in (a) vapor HF and (b) 100:1 aqueous HF.

Figure 7 shows particle counts for one typical cassette of 25 wafers. The number of particles before etching is in the range of 20–100 per wafer. The average number of particles

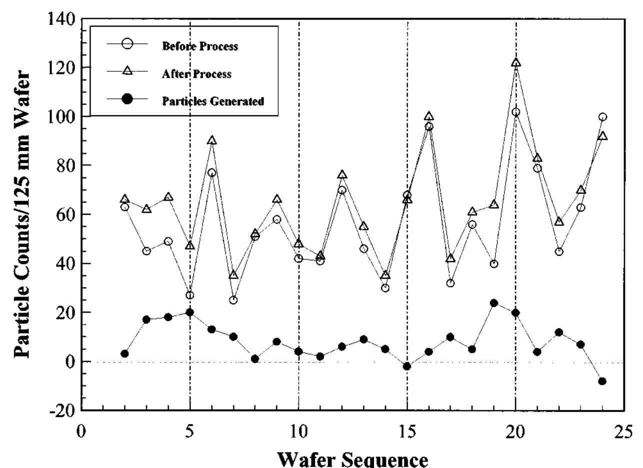

FIG. 7. Particle counts from a cassette of samples etched with vapor HF. Particles with dimension of larger than 0.2 μm were measured.

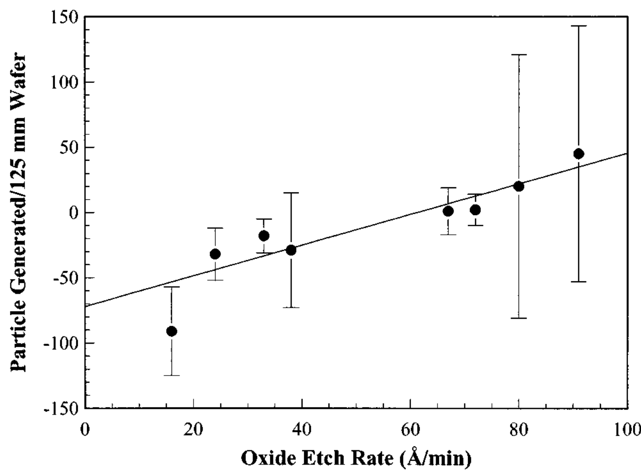

FIG. 8. Particle generation rate as a function of oxide etch rate. Oxide etching was processed at a temperature of 50 °C and a pressure of 200 Torr.

generated per wafer during the process is about eight, most of which have a diameter less than 0.3 μm. Particle generation is correlated to process temperature and oxide etch rate. We have observed less particle generation at higher temperature, since a higher by-product desorption rate is expected to result in fewer particles.

Figure 8 shows particle generation dependence on oxide etch rate. All SiO_2 etching was processed at a temperature of 50 °C and a pressure of 200 Torr. The different oxide etch rates were realized by varying the flow rates of vapor HF and methanol. We note that for etch rates lower than about 50 Å/min, the number of particles on the surface are actually reduced. However, at an etch rate of 80–100 Å/min, particles begin to accumulate on the reactive surface. At higher etching rates, by-product production may be higher than the desorption rate, resulting in particle accumulation. Lower oxide etch rate is therefore more desirable.

D. Metallic contamination removal using UV/Cl_2

Metallic contamination can severely degrade device performance. It can increase the current leakage at the $p-n$ junction, decrease the oxide breakdown field and shorten the minority carrier lifetime.[20] Some sources of contamination may be manufacturing processes such as reactive ion etching (RIE), or ion implantation.[21] Removal of metallic contamination is vital to achieve better device performance and higher yield.

Figure 9 shows chromium and iron surface concentrations as a function of different cleaning procedures. Procedures containing UV/Cl_2 steps demonstrate an effective metal removal capability. The chromium concentration is reduced to the detection limit of 2×10^{11} atoms/cm^2 after vapor HF etching and UV/Cl_2 process steps, whereas iron is reduced to 1×10^{11} atoms/cm^2. A single step of vapor HF etching does not remove metals from the Si surface. However, we have noted that it is effective in removing metals from the oxide surface. For example, the chromium concentration on the oxide surface is reduced from 1.1×10^{12} to 5×10^{11} atoms/cm^2 after a vapor HF etching process. The vapor HF process removes metallic contamination from the surface of native oxide while the UV/Cl_2 process removes metals from the Si surface. A combination of the two processes is essential for complete metal removal process.

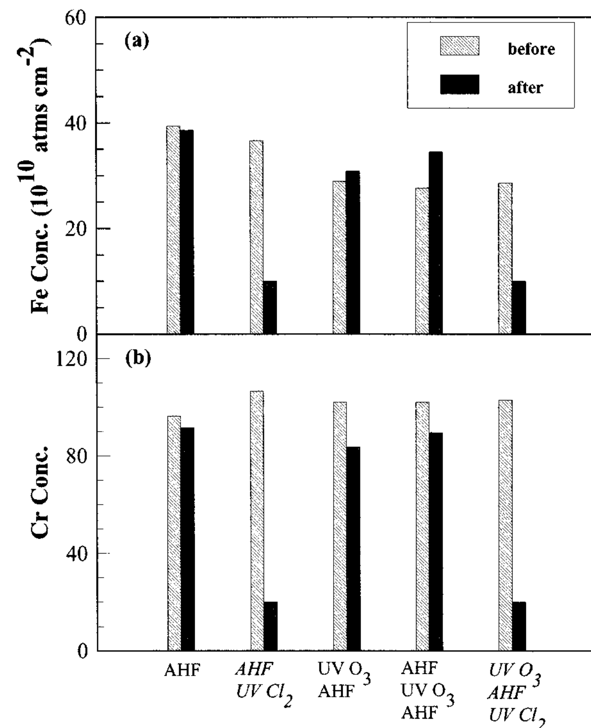

FIG. 9. (a) Iron and (b) chromium surface concentrations measured by TXRF. Among the five cleaning procedures studied, the two with UV/Cl_2 step show effective removal of trace metallic contamination.

VI. SUMMARY AND CONCLUSIONS

We have investigated the capability of vapor phase processing for pregate oxide cleaning application in a high vacuum cluster tool. Oxide etching is reproducible with a standard error from wafer to wafer under 5% for a temperature of 50 °C and chamber pressure of 200 Torr process window. No added silicon surface microroughness has been observed, even after an aggressive vapor HF etching. Particle generation during etching is about eight per wafer at an etch rate of 60 Å/min. A higher oxide etch rate normally results in greater particle deposition. Metallic contamination removal has been demonstrated via a cleaning procedure, which includes vapor HF etching, followed by an UV/Cl_2 exposure. Vapor phase cleaning technology is an important option for future cluster tool, single wafer processing development.

ACKNOWLEDGMENTS

The authors acknowledge G. Higashi for beneficial discussions; R. Keller for supplying chemical consumption data; J. Baylis of SEMATECH and I. Kashkoush of SMS for TXRF measurement; and R. Shah and G. Smolinsky of SEMATECH for funding.

[1]W. Kern, J. Electrochem. Soc. **137**, 1887 (1990).
[2]S. R. Kasi, M. Liehr, P. A. Thiry, H. Dallaporta, and M. Offenberg, Appl. Phys. Lett. **59**, 108 (1991).

[3]L. J. Huang and W. M. Lau, Appl. Phys. Lett. **60**, 1108 (1992).
[4]T. Yasuda, Y. Ma, S. Habermehl, and G. Lucovsky, Appl. Phys. Lett. **60**, 434 (1992).
[5]X. L. Xu, R. T. Kuehn, M. C. Ozturk, J. J. Wortman, R. J. Nemanich, G. S. Harris, and D. M. Maher, J. Electron. Mater. **22**, 335 (1993).
[6]B. E. Deal, M. A. McNeilly, D. B. Kao, and J. M. deLarios, *Proceedings of the First International Symposium on Cleaning Technology Semiconductor Device Manufacturing* (The Electrochemical Society, Pennington, NJ, 1989), Vol. 90-9, p. 121.
[7]J. Ruzyllo, K. Torek, C. Daffron, R. Grant, and R. Novak, J. Electrochem. Soc. **140**, L64 (1993).
[8]A. Izumi, T. Matsuka, T. Takeuchi, and A. Yamano, Proceedings of the Second International Symposium on Cleaning Technology in Semiconductor Device Manufacturing, 1991, Vol. 91, p. 260.
[9]T. Ito, R. Sugino, S. Watanabe, Y. Nara, and Y. Sato, in Ref. 6, p. 114.
[10]M. Wong, M. M. Moslehi, and R. A. Bowling, J. Electrochem. Soc. **140**, 205 (1993).
[11]R. Novak, Solid State Technol. **39** (March 1988).
[12]Y. Ma, M. L. Green, K. Torek, J. Ruzyllo, R. Opila, K. Konstadinidis, D. Siconolfi, and D. Brasen (unpublished).
[13]C. R. Helms and B. E. Deal, J. Vac. Sci. Technol. A **10**, 806 (1992).
[14]A. H. Carim and A. Bhattachayya, Appl. Phys. Lett. **46**, 872 (1985).
[15]T. Ohmi, M. Miyashita, M. Itano, T. Imaoka, and I. Kawanabe, IEEE Trans. Electron. Devices **39**, 537 (1992).
[16]T. Kitano, E. Hasegawa, M. Tsukiji, K. Akimoto, S. Kimura, S. Saito, and K. Ikeda, Jpn. J. Appl. Phys. **32**, L1581 (1993).
[17]G. S. Higashi, R. S. Becker, Y. J. Chabal, and A. J. Becker, Appl. Phys. Lett. **58**, 1656 (1991).
[18]M. Mirose, M. Hiroshima, T. Yasaka, and S. Miyasaki, J. Vac. Sci. Technol. A **12**, 1864 (1994).
[19]V. B. Menon, L. D. Michaels, R. P. Donovan, and D. S. Ensor, Solid State Technol. **32**, S7 (1989).
[20]H. Morinaga, M. Suyama, and T. Ohmi, J. Electrochem. Soc. **141**, 2834 (1994).
[21]T. Ohmi, T. Imoaka, I. Sugiyama, and T. Kezuka, J. Electrochem. Soc. **139**, 3317 (1992).